Investigating nuclear structure near $N = 32$ and $N = 34$: Precision mass measurements of neutron-rich Ca, Ti, and V isotopes

W. S. Porter,[1,2,*] E. Dunling,[1,3,†] E. Leistenschneider,[4,5,‡] J. Bergmann,[6] G. Bollen,[4,5,7] T. Dickel,[6,8] K. A. Dietrich,[1,9] A. Hamaker,[4,5,7] Z. Hockenbery,[1,10] C. Izzo,[1] A. Jacobs,[1,2] A. Javaji,[1,2] B. Kootte,[1,11] Y. Lan,[1,2] I. Miskun,[6] I. Mukul,[1] T. Murböck,[1] S. F. Paul,[1,9] W. R. Plaß,[6,8] D. Puentes,[4,5,7] M. Redshaw,[5,12] M. P. Reiter,[1,6,13] R. Ringle,[4,5] J. Ringuette,[1,14] R. Sandler,[12] C. Scheidenberger,[6,8,15] R. Silwal,[1,§] R. Simpson,[1,2] C. S. Sumithrarachchi,[4,5] A. Teigelhöfer,[1] A. A. Valverde,[11] R. Weil,[2] I. T. Yandow,[4,5,7] J. Dilling,[1,2] and A. A. Kwiatkowski[1,16]

[1]*TRIUMF, 4004 Wesbrook Mall, Vancouver, British Columbia V6T 2A3, Canada*
[2]*Department of Physics and Astronomy, University of British Columbia, Vancouver, British Columbia V6T 1Z1, Canada*
[3]*Department of Physics, University of York, York YO10 5DD, United Kingdom*
[4]*Facility for Rare Isotope Beams, Michigan State University, East Lansing, Michigan 48824, USA*
[5]*National Superconducting Cyclotron Laboratory, Michigan State University, East Lansing, Michigan 48824, USA*
[6]*II. Physikalisches Institut, Justus-Liebig-Universität, 35392 Gießen, Germany*
[7]*Department of Physics and Astronomy, Michigan State University, East Lansing, Michigan 48824, USA*
[8]*GSI Helmholtzzentrum für Schwerionenforschung GmbH, Planckstraße 1, 64291 Darmstadt, Germany*
[9]*Ruprecht-Karls-Universität Heidelberg, D-69117 Heidelberg, Germany*
[10]*Department of Physics, McGill University, 3600 Rue University, Montréal, QC H3A 2T8, Canada*
[11]*Department of Physics and Astronomy, University of Manitoba, Winnipeg, Manitoba R3T 2N2, Canada*
[12]*Department of Physics, Central Michigan University, Mount Pleasant, Michigan 48859, USA*
[13]*School of Physics and Astronomy, University of Edinburgh, Edinburgh EH9 3FD, United Kingdom*
[14]*Department of Physics, Colorado School of Mines, Golden, Colorado 80401, USA*
[15]*Helmholtz Forschungsakademie Hessen für FAIR (HFHF), GSI Helmholtzzentrum für Schwerionenforschung, Campus Gießen, 35392 Gießen, Germany*
[16]*Department of Physics and Astronomy, University of Victoria, Victoria, British Columbia V8P 5C2, Canada*

(Received 30 June 2022; accepted 29 July 2022; published 10 August 2022)

Nuclear mass measurements of isotopes are key to improving our understanding of nuclear structure across the chart of nuclides, in particular, for the determination of the appearance or disappearance of nuclear shell closures. We present high-precision mass measurements of neutron-rich Ca, Ti, and V isotopes performed at TRIUMF's Ion Trap for Atomic and Nuclear science (TITAN) and the Low Energy Beam and Ion Trap (LEBIT) facilities. These measurements were made using the TITAN multiple-reflection time-of-flight mass spectrometer (MR-ToF-MS) and the LEBIT 9.4T Penning trap mass spectrometer. In total, 13 masses were measured, 8 of which represent increases in precision over previous measurements. These measurements refine trends in the mass surface around $N = 32$ and $N = 34$, and support the disappearance of the $N = 32$ shell closure with increasing proton number. Additionally, our data do not support the presence of a shell closure at $N = 34$.

DOI: 10.1103/PhysRevC.106.024312

I. INTRODUCTION

The structure of nuclei far from stability is of primary interest within low-energy nuclear physics. The nuclear shell model has long been established as the backbone of isotopic structure, correctly reproducing the canonical magic numbers ($N, Z = 2, 8, 20, 28, 50, 82$) for protons and neutrons for spherical-like nuclei. Outside of these established points of strongest binding, magic behavior has appeared and disappeared at many asymmetric proton-to-neutron ratios [1,2]. The establishment of shell closures across the chart of nuclides is critical in part for the benchmarking of nuclear theories [3,4].

Previous experimental and theoretical studies have confirmed the presence of a closed shell at $N = 32$ near the proton $Z = 20$ shell. In particular, large 2^+ excitation energies [5,6], small $B(E2; 0^+ \rightarrow 2^+)$ [7,8] and nuclear mass trends [9–11] have all indicated the presence of a subshell at $N = 32$. Nuclear theories have corroborated experimental findings of such a subshell as well [12–14].

The existence of a similar subshell at $N = 34$ remains an open question. Experimental evidence from excitation energies [15] support the presence of a subshell. However, trends

*Current address: Department of Physics and Astronomy, University of Notre Dame, Notre Dame, Indiana 46656, USA; Corresponding author: wporter@triumf.ca
†Part of doctoral thesis, University of York, published 2021.
‡Current address: CERN, 1121, Geneva 23, Switzerland.
§Current address: Department of Physics and Astronomy, Appalachian State University, Boone, North Carolina 28608.

in two-neutron separation energies from mass measurements, most recently of Sc isotopes in [11], generally do not support the existence of such a subshell. Data from Ref. [16] suggests the presence of the $N = 34$ subshell in the Ca isotopes, whereas current Ti and V data do not suggest such a closure in their isotope chains. More precise experimental data are required in the region to establish the existence or nonexistence of an $N = 34$ subshell closure.

In this article, we present high-precision nuclear mass measurements of neutron-rich Ca, Ti, and V isotopes completed in collaboration at TRIUMF's Ion Trap for Atomic and Nuclear science (TITAN) and the Low Energy Beam and Ion Trap (LEBIT) facility at the National Superconducting Cyclotron Laboratory.

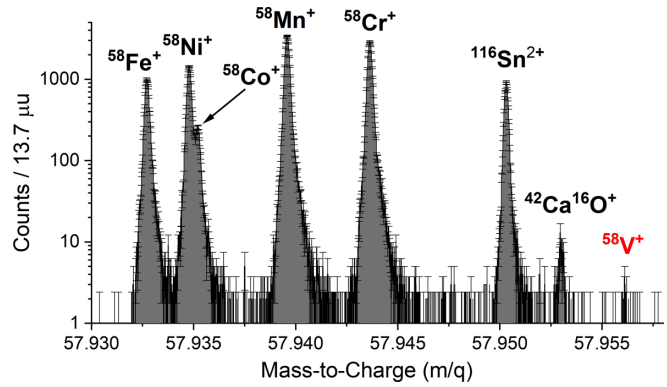

FIG. 1. A sample mass spectrum taken at $A = 58$ with the TITAN MR-ToF-MS. The identified ion species are labeled.

II. EXPERIMENT

At TRIUMF, mass measurements were performed at TITAN [17] using the multiple-reflection time-of-flight mass spectrometer (MR-ToF-MS) [18]. Isotopes of interest were produced at TRIUMF's Isotope Separator and Accelerator (ISAC) [19] where a 480-MeV 50-μA proton beam was impinged on a 22.7-g/cm^2-thick Ta target. Stopped spallation and fragmentation products diffused out of the target towards a hot Re ion source where they were surface ionized. Further ionization for Ti isotopes was achieved via TRIUMF's resonant ionization laser ion source (TRILIS), via a two-step resonant laser excitation scheme [20]. All ionized beams were sent to a mass separator which removed nonisobaric products. The isobaric beam was then transported to the TITAN facility where it was cooled and bunched via the TITAN radio-frequency quadrupole (RFQ) cooler and buncher, a linear RFQ filled with inert He gas at 10^{-2} mbar [21]. Cooled ion bunches were sent to the TITAN MR-ToF-MS for mass measurement.

The TITAN MR-ToF-MS determines the masses of ions via their time of flight over a given path and kinetic energy [22,23]. Since the mass resolution is proportional to the time-of-flight ($R = t/2\,\Delta t$), a long flight path is desired and achieved via two electrostatic mirrors. Isochronous reflection of ions by these mirrors for a sufficient number of turns achieves the desired resolution [24].

The TITAN MR-ToF-MS consists of two primary sections; a preparation section and an analyzer section. Cooled ion bunches were injected into the preparation section, which consists of a series of RFQs which further cool ion bunches for 3 ms before delivery to the analyzer section. Once inside the mass analyzer, bunches underwent between 350 and 520 isochronous turns between mirrors for a total time of flight of $\approx$10 ms before ejection onto the MagneToF detector [25] for time-of-flight detection. To minimize contaminant species in our spectra, a mass range selector consisting of two electrodes inside the mass analyzer deflected away any remaining nonisobaric beam products [26]. To measure and detect masses of very low signal-to-background ratios (< 1 to 10^4), mass-selective re-trapping was employed where ions of interest are dynamically recaptured in the injection trap after a defined flight time in the mass analyzer [27]. Recaptured ions are, subsequently, re-injected into the mass analyzer for a time-of-flight measurement. This process is highly mass selective and allows for the separation of isobaric contaminants from ions of interest during the mass measurement process [24,27–29].

Delivered beams contained many atomic and molecular contaminant species alongside the Ca, Ti, and V species of interest. An example of a mass spectrum taken during the campaign is shown in Fig. 1. An initial beam assessment was performed during the on-line experiment to identify and assign species to all peaks present in the spectrum. Species identity was confirmed by the occurrence of a species across multiple mass units. The identity of Ti in a spectrum was determined via subsequent measurements with TRILIS lasers off and on. In a lasers off measurement, one of the TRILIS lasers was blocked, removing one of the resonant excitation steps and preventing ionization of Ti. This resulted in a decrease in the overall Ti yield, and, subsequently, a decrease in time-of-flight counts of Ti in a spectrum. A large count increase ($\sim$ a factor 4) during a lasers on measurement unambiguously confirmed the identification of Ti. More details on the experimental campaign of Ca, Ti, and V masses at TITAN can be found in Ref. [30].

At the NSCL, isotopes of interest were produced via the in flight method [31] where a 130-MeV/u ^{76}Ge primary ion beam was impinged on a natural Be target $\approx$0.4 g/cm^2 thick. Desired fragments were separated from contaminants via the A1900 fragment separator [32], and progressed towards a gas catcher [33] where they were stopped as ions in a high-purity He gas. Ions were extracted from the gas catcher as a low-energy, continuous beam and transported to a dipole magnet mass separator for separation of nonisobaric products. Ions of interest, which were primarily singly charged oxides formed from interactions inside the gas catcher, were sent to theLEBIT facility [34].

Continuous beams entering the LEBIT facility were sent to a cooler and buncher for cooling, accumulation, and bunching, and released as ion bunches [35]. Bunches were delivered to the LEBIT Penning trap mass spectrometer where isobaric contaminants were cleaned away via application of a dipolar rf field [36] before the mass measurement.

Mass measurements of ions within the LEBIT Penning trap were completed via determination of the cyclotron frequency

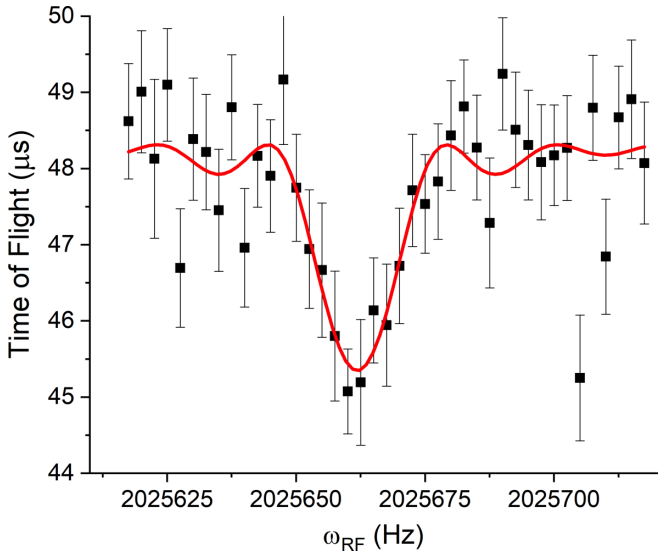

FIG. 2. A ToF-ICR spectrum taken for ^{55}Ti ^{16}O$^+$ with the LEBIT Penning trap mass spectrometer. The fit result of an analytical function described in Ref. [38], shown in red, is used to extract the minimum in time of flight that occurs at $\omega_{\rm rf} = \omega_c$.

(ω_c) of the ion around a 9.4-T magnetic field using the time-of-flight ion-cyclotron-resonance (ToF-ICR) technique [37]. In ToF-ICR, an ion's slow magnetron drift is converted into a fast modified cyclotron motion through the application of a quadrupole rf pulse at ω_{rf} near the cyclotron frequency. At $\omega_{\rm rf} = \omega_c$, and with a well-chosen duration of the rf pulse, full conversion to the fast modified cyclotron motion can be achieved, resulting in a maximum in radial kinetic energy and a minimum in time of flight to a downstream detector. Scanning $\omega_{\rm rf}$ over a series of frequencies around ω_c, results in a time-of-flight spectra with a minimum at ω_c, as seen in Fig. 2. Standard excitation schemes with rf pulse durations between 50 and 500 ms, described in more detail in Ref. [38] were used.

III. ANALYSIS

Time-of-flight spectra taken with the TITAN MR-ToF-MS are converted to mass spectra via the relationship,

$$\frac{m_{\rm ion}}{q} = C(t_{\rm ion} - t_0)^2, \tag{1}$$

where t_0 is 0.18 μs as determined offline and C is a calibration factor determined from a high-statistics well-known reference ion in each spectrum as listed in Table I. To account for time-dependent drifts of times of flight, a time-resolved calibration was performed [39] using the mass data-acquisition software package [40]. Peak centroids were determined by fitting hyper-exponentially modified Gaussian functions [41] using the EMGFIT PYTHON library [42]. Statistical uncertainties are generated based on techniques described in Refs. [39,42]. Systematic uncertainties of the MR-ToF-MS system are described in detail in Refs. [24,39], and total to a value of $\approx 2.0 \times 10^{-7}$. This uncertainty is dominated by the uncertainties due to ion-ion interactions (3.3×10^{-8} per detected ion), the nonideal switching of mirrors (7.0×10^{-8}), and a further unknown systematic error ($\approx 1.9 \times 10^{-7}$).

ToF-ICR spectra taken with the LEBIT Penning trap, e.g., Fig. 2, were fit with the analytical function described in Ref. [38] to extract the cyclotron frequency. The atomic mass is determined via the ratio,

$$R = \frac{\omega_{\rm c,ref}}{\omega_{\rm c}} = \frac{m - m_e}{m_{\rm ref} - m_e}, \tag{2}$$

where m_e is the mass of the electron, ω_c and m the cyclotron frequency and mass of the ion of interest, and $\omega_{\rm c,ref}$ and $m_{\rm ref}$ the cyclotron frequency and mass of a reference ion. Reference ions were required to have well-known literature masses (with values taken from Ref. [43]) and the same A/q as the ion of interest and were measured either before or after ion-of-interest measurements to account for potential fluctuations of the magnetic field. Ionization potentials and molecular binding energies are not considered in any of our mass determinations as they are smaller than 20 eV and do not contribute at the level of precision we attain. Systematic

TABLE I. Results of the mass measurements performed, compared to the values recommended by AME2020 [43]. Included is the mass ratio ($m_{\rm ionic,IOI}/m_{\rm ionic,ref}$) between the ionic masses of the ion of interest (IOI) and the reference ion for all measurements. Differences are $m_{\rm new} - m_{\rm lit}$. All mass values are in keV. All TITAN and LEBIT measurements were measured as singly charged ions.

Facility	Nuclide	Mass excess	Literature	Difference	Reference ion	Mass ratio
TITAN	^{54}Ca	−25119(12)	−25160(50)	41(51)	^{54}Cr$^+$	1.000 633 250 (239)
LEBIT	^{52}Ti	−49478.6(2.2)	−49477.7(2.7)	−0.9(3.5)	^{48}Ti ^{16}O$^+$	0.999 979 3643 (887)
TITAN	^{54}Ti	−45738(27)	−45744(16)	6(31)	^{54}Cr$^+$	1.000 222 872 (546)
LEBIT	^{55}Ti	−41827.0(5.7)	−41832(29)	5(30)	^{46}Ti ^{19}F$^+$	0.999 922 402 (133)
TITAN	^{55}Ti	−41815(22)	−41832(29)	17(36)	^{55}Cr$^+$	1.000 259 788 (428)
TITAN	^{56}Ti	−39390(21)	−39420(100)	30(102)	^{56}Cr$^+$	1.000 305 043 (401)
TITAN	^{54}V	−49899(10)	−49898(11)	−1(15)	^{54}Cr$^+$	1.000 140 049 (195)
TITAN	^{55}V	−49138.2(6.6)	−49125(27)	−13(28)	^{55}Cr$^+$	1.000 116 697 (129)
TITAN	^{56}V	−46268(14)	−46180(180)	−88(181)	^{56}Cr$^+$	1.000 173 049 (274)
LEBIT	^{56}V	−46198(36)	−46180(180)	−18(184)	^{34}S ^{19}F$_2^+$	0.999 731 060 (540)
TITAN	^{57}V	−44382.4(8.3)	−44440(80)	58(80)	^{57}Cr$^+$	1.000 153 511 (161)
LEBIT	^{57}V	−44371(15)	−44440(80)	69(81)	^{12}C$_3$ ^{1}H$_5$ ^{16}O$_2^+$	0.998 881 613 (220)
TITAN	^{58}V	−40361(44)	−40430(100)	69(109)	^{58}Fe$^+$	1.000 403 867 (820)

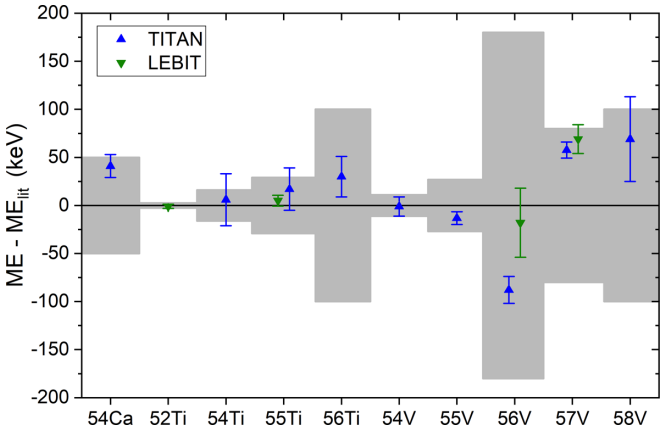

FIG. 3. A plot comparing mass values from Ref. [43] to experimental mass results from this paper. Gray bands represent error bars given on values in Ref. [43].

uncertainties, for example, arising from a small misalignment of the trapping axis and the magnetic field, or small deviations from a perfect quadrupole electric potential were determined to contribute at the $\approx 10^{-10}$ level and, thus, were negligible [44].

IV. RESULTS

Table I reports the masses of all isotopes measured in this paper as well their mass excesses as found in literature. Figure 3 compares our mass results to data presented in Ref. [43]. All masses had been previously measured in some capacity to varying precisions; our measurements are in agreement with the earlier results within 0.9σ. Our measurements of ^{54}Ca, ^{52}Ti, ^{55}Ti, ^{56}Ti, ^{55}V, ^{56}V, ^{57}V, and ^{58}V represent an increase in precision over previous values with all but two of these representing a precision increase of a factor of 2 or more.

Mass measurements of ^{55}Ti, ^{56}V, and ^{57}V were completed at both facilities with results from both campaigns reported in Table I. The reported measurements for ^{55}Ti, ^{56}V, and ^{57}V agree to 0.5σ, 1.8σ, and 0.7σ, respectively.

In order to probe the shell structure in the region encompassed by our measurements, we consider the two-neutron separation energies (S_{2n}), defined as

$$S_{2n}(N,Z) = m(N-2,Z) + 2m_n - m(N,Z), \qquad (3)$$

with $m(N,Z)$ the mass excess and m_n the mass of the neutron. Figure 4 shows S_{2n} values for the $Z = 19$–24 isotopes. Our results show that the steep drop off at $N = 32$ seen in the Ca and Sc isotopes chains is not present in the Ti and V chains. This confirms the disappearance of the $N = 32$ shell closure at and above $Z = 22$ as presented in Ref. [13]. No drop off is seen at $N = 34$ for any of the presented isotope chains.

To further probe the structures seen in separation energy trends, we consider the empirical shell gap parameter (δ_{2n}), given as

$$\delta_{2n} = S_{2n}(N,Z) - S_{2n}(N+2,Z). \qquad (4)$$

Figure 5 shows δ_{2n} for the $Z = 19$–24 isotopes. As a pseudoderivative of S_{2n}, low-δ_{2n} values decreasing towards zero

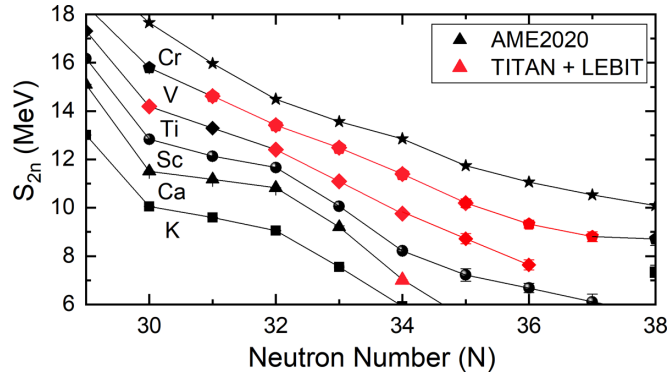

FIG. 4. A graph of the S_{2n} in the $Z = 19$–24 isotope chains based on mass values from Ref. [43] (black symbols), and Ca, Ti, and V mass measurements from this paper (red symbols). For the cases of ^{55}Ti, ^{56}V, and ^{57}V where both TITAN and LEBIT measured a mass value, the more precise mass value was used in the determination of the plotted S_{2n} value.

indicate a flattening in S_{2n}, whereas a sharp peak indicates a steep drop off in S_{2n} at N. Such sharp peaks, when at even neutron numbers, are typically indicative of shell closures [13]. A decrease in δ_{2n} from Ca towards V is seen at $N = 32$, strongly signaling the disappearance of the $N = 32$ shell closure. Additionally, our data do not show any peaklike behavior at $N = 34$ and, thus, does not support the presence of a shell closure at $N = 34$. However, mass measurements of more neutron-rich isotopes are needed to extend the mass surface and fully characterize the region surrounding $N = 34$.

A comparison of our results to recent calculations using the valence-space in-medium similarity renormalization group

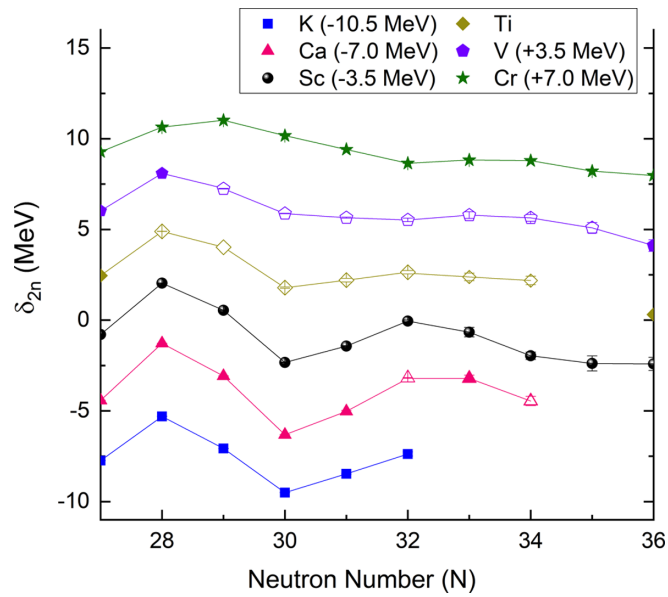

FIG. 5. A graph of the δ_{2n} for the $Z = 19$–24 isotope chains. Values are offset by amounts as presented in the legend. Unfilled symbols represent values from this paper. The disappearance of a peak at $N = 32$, signifying the disappearance of a shell closure at $N = 32$, can be seen as the proton number increases.

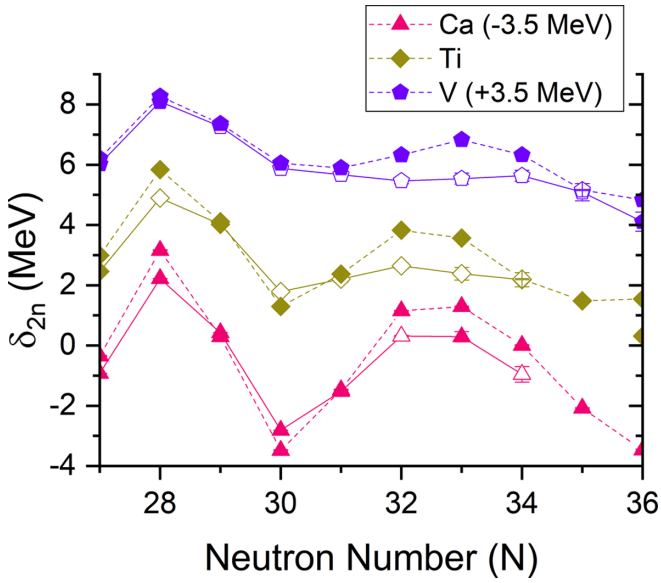

FIG. 6. A graph comparing δ_{2n} experimental values (solid lines) to theoretical calculations (dashed lines) from Ref. [45]. Values are offset by amounts as presented in the legend. Unfilled symbols represent values from this paper.

(VS-IMSRG) [45] is presented in Fig. 6. The VS-IMSRG calculations generally overshoot the experimental results but follow the overall trends seen in the mass surface, including the disappearance of the $N = 32$ shell closure at higher proton numbers. Additionally, no evidence for a $N = 34$ shell closure is seen in the calculations. More refinement of *ab initio* calculations is ultimately needed for a complete picture of the $N = 32$ and $N = 34$ regions.

V. SUMMARY

Measurements of neutron-rich Ca, Ti, and V isotopes were performed at the TITAN facility in Canada using its MR-ToF-MS and the LEBIT facility in the United States using its Penning trap mass spectrometer. These results, totaling 13 mass measurements, include 8 masses which increase precisions with respect to previous measurements. These measurements refine the nuclear mass surface around $N = 32$ and $N = 34$ and confirm the waning of the $N = 32$ shell closure as $Z = 20$ is exceeded. The refined mass surface also does not support the presence of an $N = 34$ shell closure. Mass data on more neutron-rich nuclides are ultimately needed to further understand the nuclear structure of the region.

ACKNOWLEDGMENTS

We would like to thank J. Lassen and the laser ion source group at TRIUMF for their development of the relevant laser scheme as well as the NSCL staff, the ISAC Beam Delivery group, and M. Good for their technical support. This work was supported by the Natural Sciences and Engineering Research Council (NSERC) of Canada under Grants No. SAPIN-2018-00027, No. RGPAS-2018-522453, and No. SAPPJ-2018-00028, the National Research Council (NRC) of Canada through TRIUMF, the U.S. National Science Foundation through Grants No. PHY-1565546, No. PHY-2111185, and No. PHY-1811855, the U.S. Department of Energy, Office of Science under Grants No. DE-FG02-93ER40789 and No. DE-SC0015927, the German Research Foundation (DFG), Grant No. SCHE 1969/2-1, the German Federal Ministry for Education and Research (BMBF), Grants No. 05P19RGFN1 and No. 05P21RGFN1, and the Hessian Ministry for Science and Art through the LOEWE Center HICforFAIR, by the JLU and GSI under the JLU-GSI strategic Helmholtz partnership agreement. E.D. acknowledges financial support from the U.K.-Canada Foundation.

[1] I. Tanihata, H. Hamagaki, O. Hashimoto, Y. Shida, N. Yoshikawa, K. Sugimoto, O. Yamakawa, T. Kobayashi, and N. Takahashi, Measurements of Interaction Cross Sections and Nuclear Radii in the Light *p*-Shell Region, Phys. Rev. Lett. **55**, 2676 (1985).

[2] R. Kanungo, A new view of nuclear shells, Phys. Scr. **2013**, 014002 (2013).

[3] A. I. Georgieva, A. Aprahamian, I. Bentley, A. Teymurazyan, and A. Nystrom, Systematic evaluation of the nuclear binding energies as functions of f-spin, Bulgarian Journal of Physics (Print) **42**, 544 (2015).

[4] J. Simonis, K. Hebeler, J. D. Holt, J. Menéndez, and A. Schwenk, Exploring *sd*-shell nuclei from two- and three-nucleon interactions with realistic saturation properties, Phys. Rev. C **93**, 011302(R) (2016).

[5] A. Huck, G. Klotz, A. Knipper, C. Miehé, C. Richard-Serre, G. Walter, A. Poves, H. L. Ravn, and G. Marguier, Beta decay of the new isotopes ^{52}K, ^{52}Ca, and ^{52}Sc; a test of the shell model far from stability, Phys. Rev. C **31**, 2226 (1985).

[6] M. L. Cortés, W. Rodriguez, P. Doornenbal, A. Obertelli, J. D. Holt, J. Menéndez, K. Ogata, A. Schwenk, N. Shimizu, J. Simonis, Y. Utsuno, K. Yoshida, L. Achouri, H. Baba, F. Browne, D. Calvet, F. Château, S. Chen, N. Chiga, A. Corsi *et al.*, $N = 32$ shell closure below calcium: Low-lying structure of ^{50}Ar, Phys. Rev. C **102**, 064320 (2020).

[7] M. Seidlitz, P. Reiter, A. Dewald, O. Möller, B. Bruyneel, S. Christen, F. Finke, C. Fransen, M. Górska, H. Grawe, A. Holler, G. Ilie, T. Kotthaus, P. Kudejová, S. M. Lenzi, S. Mandal, B. Melon, D. Mücher, J.-M. Regis, B. Saha *et al.*, Precision lifetime measurements of the first 2^+ and 4^+ states in ^{56}Cr at the $N = 32$ subshell closure, Phys. Rev. C **84**, 034318 (2011).

[8] A. Goldkuhle, A. Goldkuhle, C. Fransen, A. Blazhev, M. Beckers, B. Birkenbach, T. Braunroth, E. Clément, A. Dewald, J. Dudouet, J. Eberth, H. Hess, B. Jacquot, J. Jolie, Y.-H. Kim, A. Lemasson, S. M. Lenzi, H. J. Li, J. Litzinger, C. Michelagnoli *et al.*, Lifetime measurements in ^{52,54}Ti to study shell evolution toward $N = 32$, Phys. Rev. C **100**, 054317 (2019).

[9] F. Wienholtz, D. Beck, K. Blaum, C. Borgmann, M. Breitenfeldt, R. B. Cakirli, S. George, F. Herfurth, J. D. Holt, M. Kowalska, S. Kreim, D. Lunney, V. Manea, J. Menéndez, D. Neidherr, M. Rosenbusch, L. Schweikhard, A. Schwenk, J. Simonis, J. Stanja *et al.*, Masses of exotic calcium isotopes pin down nuclear forces, Nature (London) **498**, 346 (2013).

[10] M. P. Reiter, S. Ayet San Andrés, E. Dunling, B. Kootte, E. Leistenschneider, C. Andreoiu, C. Babcock, B. R. Barquest, J. Bollig, T. Brunner, I. Dillmann, A. Finlay, G. Gwinner, L. Graham, J. D. Holt, C. Hornung, C. Jesch, R. Klawitter, Y. Lan, D. Lascar *et al.*, Quenching of the $N = 32$ neutron shell closure studied via precision mass measurements of neutron-rich vanadium isotopes, Phys. Rev. C **98**, 024310 (2018).

[11] E. Leistenschneider, E. Dunling, G. Bollen, B. A. Brown, J. Dilling, A. Hamaker, J. D. Holt, A. Jacobs, A. A. Kwiatkowski, T. Miyagi, W. S. Porter, D. Puentes, M. Redshaw, M. P. Reiter, R. Ringle, R. Sandler, C. S. Sumithrarachchi, A. A. Valverde, and I. T. Yandow (The LEBIT Collaboration and the TITAN Collaboration) Precision Mass Measurements of Neutron-Rich Scandium Isotopes Refine the Evolution of $N = 32$ and $N = 34$ Shell Closures, Phys. Rev. Lett. **126**, 042501 (2021).

[12] T. Otsuka, Y. Utsuno, M. Honma, and T. Mizusaki, Structure of unstable nuclei, Prog. Part. Nucl. Phys. **46**, 155 (2001).

[13] E. Leistenschneider, M. P. Reiter, S. Ayet San Andrés, B. Kootte, J. D. Holt, P. Navrátil, C. Babcock, C. Barbieri, B. R. Barquest, J. Bergmann, J. Bollig, T. Brunner, E. Dunling, A. Finlay, H. Geissel, L. Graham, F. Greiner, H. Hergert, C. Hornung, C. Jesch *et al.*, Dawning of the $N = 32$ Shell Closure Seen through Precision Mass Measurements of Neutron-Rich Titanium Isotopes, Phys. Rev. Lett. **120**, 062503 (2018).

[14] J. G. Li, B. S. Hu, Q. Wu, Y. Gao, S. J. Dai, and F. R. Xu, Neutron-rich calcium isotopes within realistic Gamow shell model calculations with continuum coupling, Phys. Rev. C **102**, 034302 (2020).

[15] D. Steppenbeck, S. Takeuchi, N. Aoi, P. Doornenbal, M. Matsushita, H. Wang, H. Baba, N. Fukuda, S. Go, M. Honma, J. Lee, K. Matsui, S. Michimasa, T. Motobayashi, D. Nishimura, T. Otsuka, H. Sakurai, Y. Shiga, P.-A. Söderström, T. Sumikama *et al.*, Evidence for a new nuclear magic number' from the level structure of ^{54}Ca, Nature (London) **502**, 207 (2013).

[16] S. Michimasa, M. Kobayashi, Y. Kiyokawa, S. Ota, D. S. Ahn, H. Baba, G. P. A. Berg, M. Dozono, N. Fukuda, T. Furuno, E. Ideguchi, N. Inabe, T. Kawabata, S. Kawase, K. Kisamori, K. Kobayashi, T. Kubo, Y. Kubota, C. S. Lee, M. Matsushita *et al.*, Magic Nature of Neutrons in ^{54}Ca: First Mass Measurements of $^{55-57}$Ca, Phys. Rev. Lett. **121**, 022506 (2018).

[17] J. Dilling, R. Baartman, P. Bricault, M. Brodeur, L. Blomeley, F. Buchinger, J. Crawford, J. R. Crespo López-Urrutia, P. Delheij, M. Froese, G. P. Gwinner, Z. Ke, J. K. Lee, R. B. Moore, V. Ryjkov, G. Sikler, M. Smith, J. Ullrich, and J. Vaz, Mass measurements on highly charged radioactive ions, a new approach to high precision with TITAN, Int. J. Mass Spectrom. **251**, 198 (2006).

[18] C. Jesch, T. Dickel, W. R. Plaß, D. Short, S. Ayet San Andres, J. Dilling, H. Geissel, F. Greiner, J. Lang, K. G. Leach, W. Lippert, C. Scheidenberger, and M. I. Yavor, The MR-TOF-MS isobar separator for the TITAN facility at TRIUMF, Hyperfine Interact. **235**, 97 (2015).

[19] G. C. Ball, G. Hackman, and R. Krücken, The TRIUMF-ISAC facility: two decades of discovery with rare isotope beams, Phys. Scr. **91**, 093002 (2016).

[20] J. Lassen, R. Li, S. Raeder, X. Zhao, T. Dekker, H. Heggen, P. Kunz, C. D. P. Levy, M. Mostanmand, A. Teigelhöfer, and F. Ames, Current developments with TRIUMF's titanium-sapphire laser based resonance ionization laser ion source, Hyperfine Interact. **238**, 33 (2017).

[21] T. Brunner, M. J. Smith, M. Brodeur, S. Ettenauer, A. T. Gallant, V. V. Simon, A. Chaudhuri, A. Lapierre, E. Mané, R. Ringle, M. C. Simon, J. A. Vaz, P. Delheij, M. Good, M. R. Pearson, and J. Dilling, TITAN's digital RFQ ion beam cooler and buncher, operation and performance, Nucl. Instrum. Methods Phys. Res., Sect. A **676**, 32 (2012).

[22] H. Wollnikand M. Przewloka, Time-of-flight mass spectrometers with multiply reflected ion trajectories, Int. J. Mass Spectrom. Ion Processes **96**, 267 (1990).

[23] W. R. Plaß, T. Dickel, and C. Scheidenberger, Multiple-reflection time-of-flight mass spectrometry, Int. J. Mass Spectrom. **349**, 134 (2013).

[24] M. P. Reiter, S. A. S. Andrés, J. Bergmann, T. Dickel, J. Dilling, A. Jacobs, A. A. Kwiatkowski, W. R. Plaß, C. Scheidenberger, D. Short, C. Will, C. Babcock, E. Dunling, A. Finlay, C. Hornung, C. Jesch, R. Klawitter, B. Kootte, D. Lascar, E. Leistenschneider *et al.*, Commissioning and performance of TITAN's Multiple-Reflection Time-of-Flight Mass-Spectrometer and isobar separator, Nucl. Instrum. Methods Phys. Res., Sect. A **1018**, 165823 (2021).

[25] D. Stresau, K. Hunter, W. Shiels, P. Raffin, and Y. Benari, A New Class of Robust Sub-nanosecond TOF Detectors with High Dynamic Range.

[26] T. Dickel, W. R. Plaß, A. Becker, U. Czok, H. Geissel, E. Haettner, C. Jesch, W. Kinsel, M. Petrick, C. Scheidenberger, A. Simon, and M. I. Yavor, A high-performance multiple-reflection time-of-flight mass spectrometer and isobar separator for the research with exotic nuclei, Nucl. Instrum. Methods Phys. Res., Sect. A **777**, 172 (2015).

[27] T. Dickel, W. R. Plaß, W. Lippert, J. Lang, M. I. Yavor, H. Geissel, and C. Scheidenberger, Isobar Separation in a Multiple-Reflection Time-of-Flight Mass Spectrometer by Mass-Selective Re-Trapping, J. Am. Soc. Mass Spectrom. **28**, 1079 (2017).

[28] S. Beck, B. Kootte, I. Dedes, T. Dickel, A. Kwiatkowski, E. M. Lykiardopoulou, W. R. Plaß, M. P. Reiter, C. Andreoiu, J. Bergmann, T. Brunner, D. Curien, J. Dilling, J. Dudek, E. Dunling, J. Flowerdew, A. Gaamouci, L. Graham, G. Gwinner, A. Jacobs *et al.*, Mass Measurements of Neutron-Deficient Yb Isotopes and Nuclear Structure at the Extreme Proton-Rich Side of the $N = 82$ Shell, Phys. Rev. Lett. **127**, 112501 (2021).

[29] C. Izzo, J. Bergmann, K. A. Dietrich, E. Dunling, D. Fusco, A. Jacobs, B. Kootte, G. Kripkó-Koncz, Y. Lan, E. Leistenschneider, E. M. Lykiardopoulou, I. Mukul, S. F. Paul, M. P. Reiter, J. L. Tracy, Jr., C. Andreoiu, T. Brunner, T. Dickel, J. Dilling, I. Dillmann *et al.*, Mass measurements of neutron-rich indium isotopes for r-process studies, Phys. Rev. C **103**, 025811 (2021).

[30] E. Dunling, Exploring magicity around $N = 32$ and 34 in $Z \geqslant 20$ isotopes via precision mass measurements and developments with the TITAN MR-TOF mass spectrometer, Ph.D. thesis, University of York, 2021.

[31] J. Äystö, Development and applications of the IGISOL technique, Nucl. Phys. A **693**, 477 (2001).

[32] D. J. Morrissey, B. M. Sherrill, M. Steiner, A. Stolz, and I. Wiedenhoever, Commissioning the A1900 projectile fragment

separator, Nucl. Instrum. Methods Phys. Res., Sect. B **204**, 90 (2003).

[33] C. S. Sumithrarachchi, D. J. Morrissey, S. Schwarz, K. Lund, G. Bollen, R. Ringle, G. Savard, and A. C. Villari, Beam thermalization in a large gas catcher, Nucl. Instrum. Methods Phys. Res., Sect. B **463**, 305 (2020).

[34] R. Ringle, S. Schwarz, and G. Bollen, Penning trap mass spectrometry of rare isotopes produced via projectile fragmentation at the lebit facility, Int. J. Mass Spectrom. **349**, 87 (2013), 100 years of Mass Spectrometry.

[35] S. Schwarz, G. Bollen, R. Ringle, J. Savory, and P. Schury, The LEBIT ion cooler and buncher, Nucl. Instrum. Methods Phys. Res., Sect. A **816**, 131 (2016).

[36] A. A. Kwiatkowski, G. Bollen, M. Redshaw, R. Ringle, and S. Schwarz, Isobaric beam purification for high precision Penning trap mass spectrometry of radioactive isotope beams with SWIFT, Int. J. Mass Spectrom. **379**, 9 (2015).

[37] J. Dilling, K. Blaum, M. Brodeur, and S. Eliseev, Penning-Trap Mass Measurements in Atomic and Nuclear Physics, Annu. Rev. Nucl. Part. Sci. **68**, 45 (2018).

[38] M. König, G. Bollen, H. J. Kluge, T. Otto, and J. Szerypo, Quadrupole excitation of stored ion motion at the true cyclotron frequency, Int. J. Mass Spectrom. Ion Processes **142**, 95 (1995).

[39] S. Ayet San Andrés, C. Hornung, J. Ebert, W. R. Plaß, T. Dickel, H. Geissel, C. Scheidenberger, J. Bergmann, F. Greiner, E. Haettner, C. Jesch, W. Lippert, I. Mardor, I. Miskun, Z. Patyk, S. Pietri, A. Pihktelev, S. Purushothaman, M. P. Reiter, A.-K. Rink *et al.*, High-resolution, accurate multiple-reflection time-of-flight mass spectrometry for short-lived, exotic nuclei of a few events in their ground and low-lying isomeric states, Phys. Rev. C **99**, 064313 (2019).

[40] T. Dickel, S. A. San Andrés, S. Beck, J. Bergmann, J. Dilling, F. Greiner, C. Hornung, A. Jacobs, G. Kripko-Koncz, A. Kwiatkowski, E. Leistenschneider, A. Pikthtelev, W. R. Plaß, M. P. Reiter, C. Scheidenberger, C. Will, and f. t. T. Collaboration, Recent upgrades of the multiple-reflection time-of-flight mass spectrometer at TITAN, TRIUMF, Hyperfine Interact. **240**, 62 (2019).

[41] S. Purushothaman, S. Ayet San Andrés, J. Bergmann, T. Dickel, J. Ebert, H. Geissel, C. Hornung, W. R. Plaß, C. Rappold, C. Scheidenberger, Y. K. Tanaka, and M. I. Yavor, Hyper-EMG: A new probability distribution function composed of Exponentially Modified Gaussian distributions to analyze asymmetric peak shapes in high-resolution time-of-flight mass spectrometry, Int. J. Mass Spectrom. **421**, 245 (2017).

[42] S. F. Paul, emgfit - Fitting of time-of-flight mass spectra with hyper-EMG models (2021).

[43] M. Wang, W. Huang, F. Kondev, G. Audi, and S. Naimi, The AME 2020 atomic mass evaluation (II). Tables, graphs and references*, Chin. Phys. C **45**, 030003 (2021).

[44] K. Gulyuz, J. Ariche, G. Bollen, S. Bustabad, M. Eibach, C. Izzo, S. J. Novario, M. Redshaw, R. Ringle, R. Sandler, S. Schwarz, and A. A. Valverde, Determination of the direct double-β-decay q value of ^{96}Zr and atomic masses of $^{90-92,94,96}$Zr and $^{92,94-98,100}$Mo, Phys. Rev. C **91**, 055501 (2015).

[45] S. R. Stroberg, J. D. Holt, A. Schwenk, and J. Simonis, *Ab Initio* Limits of Atomic Nuclei, Phys. Rev. Lett. **126**, 022501 (2021).